biology

MDPI

Article

Comparative Characterization of Extracellular-Vesicle-Enriched Fractions from Fresh Salivary Gland Secretions and Lyophilized Head Tissue of *Hirudo nipponia*

Meng-Xiang Jia, Ya-Li Zhu, Xia Qiu, Qian Li, Wei-Min Wang and Yuan-Yuan Luo *

College of Life Sciences, China Jiliang University, Hangzhou 310018, China; 15626948625@163.com (M.-X.J.); zhuyali021@163.com (Y.-L.Z.); qiu999@cjlu.edu.cn (X.Q.); liq2014@cjlu.edu.cn (Q.L.); wwm@cjlu.edu.cn (W.-M.W.)
* Correspondence: yyluo@cjlu.edu.cn

Simple Summary

Medicinal leeches have been employed in clinical practice for over two millennia, particularly to facilitate post-surgical recovery. This therapeutic application is attributed to bioactive compounds in leech saliva—most notably anticoagulants such as hirudin—and anti-inflammatory agents that collectively mitigate thrombosis and tissue edema. Nevertheless, the precise mechanisms underlying the systemic delivery and functional modulation of these bioactive molecules remain incompletely elucidated. Recent advances in intercellular communication have highlighted extracellular vesicles (EVs)—endogenous, lipid bilayer-enclosed nanoparticles secreted by cells—as critical mediators of intercellular signaling and targeted molecular transport. Given their biocompatibility, low immunogenicity, and natural cargo-loading capacity, EVs are increasingly investigated as next-generation delivery platforms for biologics. In this study, we systematically characterized EV-like particles isolated from two anatomical sources of the medicinal leech *Hirudo nipponia*: freshly excised salivary glands and lyophilized cephalic tissue. Using transmission electron microscopy, nanoparticle tracking analysis, and high-resolution mass spectrometry, we confirmed the presence of morphologically and biophysically consistent EVs in both preparations. Proteomic profiling revealed that these particles encapsulate six well-characterized therapeutic proteins native to leech saliva, including hirudin, destabilase, bdellin, eglin, apyrase, and hyaluronidase. Collectively, these findings demonstrate that leech-derived bioactivity is mediated not solely by freely diffusible effectors but also by extracellular vesicles carrying functional protein cargo. This study provides a proteomic foundation for understanding the delivery mechanisms of leech therapeutic molecules and lays preliminary groundwork for further research into leech-derived EVs as natural bioactive carriers.

Check for updates

Academic Editor: Sigrun Lange

Received: 27 October 2026
Revised: 24 November 2026
Accepted: 26 November 2026
Published: 29 November 2026

Copyright: © 2026 by the authors. Licensee MDPI, Basel, Switzerland. This article is an open access article distributed under the terms and conditions of the Creative Commons Attribution (CC BY) license.

Abstract

Extracellular vesicles (EVs), as endogenous mediators of intercellular communication, have been extensively characterized in mammalian systems; however, EVs from non-mammalian medicinal organisms remain comparatively undercharacterized. Despite the well-established medicinal value of the invertebrate *H. nipponia*—largely attributed to the complex bioactive secretions of its salivary glands—the characterization of its salivary gland-derived extracellular vesicles has yet to be fully explored, with current studies still in the nascent stages. In this study, four types of extracellular vesicles were isolated from the salivary glands of living *H. nipponia* and the heads of lyophilized *H. nipponia* using differential ultracentrifugation. Their morphological features and particle size distributions were characterized via transmission electron microscopy (TEM) and nanoparticle tracking

analysis (NTA), respectively. Finally, their protein compositions were comprehensively analyzed using proteomic techniques. Characterization by TEM and NTA confirmed that large extracellular vesicles (lEVs) and small extracellular vesicle (sEVs) from both origins displayed classical saucer-like vesicular structures, with diameters consistently ranging from 100 to 300 nm. Notably, proteomic analysis indicated that EVs harvested from live *H. nipponia* salivary glands preserved a broader profile of proteins with reported pharmacological activities than the lyophilized head tissue preparations. In conclusion, the successful isolation and profiling of *H. nipponia* salivary gland-derived EVs provide a foundational framework and fresh perspectives for exploring the biological roles of extracellular vesicles in invertebrates.

Keywords: proteomics; salivary gland; lyophilized head tissue; extracellular vesicles; *Hirudo nipponia*

1. Introduction

Extracellular vesicles (EVs) are lipid bilayer-enclosed nanoscale particles released by cells into the extracellular space and function as key mediators of intercellular communication [1–3]. They participate in a wide range of physiological and pathological processes by transferring proteins, nucleic acids, and lipids between cells [4,5]. Traditionally, EVs are classified by biogenetic origin into exosomes (30–150 nm, endosome-derived) and microvesicles (100–1000 nm, plasma membrane-derived), which differ in molecular composition and functional properties [6]. However, in accordance with the latest MISEV2023 guidelines, operational nomenclature based on isolation conditions and size ranges is recommended when the biogenesis of EV subsets is not directly demonstrated [7].

In experimental practice, EVs are commonly separated into large extracellular vesicle (lEVs) and small extracellular vesicle (sEVs) fractions by differential ultracentrifugation (typically at approximately 10,000× *g* and 100,000–200,000× *g*, respectively [8]). These operational fractions do not strictly correspond to vesicles of distinct biogenetic origins [9–11].

In addition to their biological roles, EVs have attracted increasing attention as natural delivery vehicles due to their ability to transport bioactive molecules and interact with recipient cells [12,13]. However, to investigate their molecular composition and functional properties, EVs must be isolated from complex biological environments. Such isolation remains challenging, particularly in non-model organisms and heterogeneous tissue-derived samples, due to issues such as sample heterogeneity, co-isolation of non-vesicular components, and the lack of standardized purification strategies [14–16].

EVs derived from natural biological sources have recently gained interest for their potential applications, yet current research has largely focused on mammalian cell-derived and plant-derived EVs. For example, mammalian mesenchymal stem cell-derived EVs are extensively utilized in tissue engineering to promote fibroblast proliferation and wound healing [17,18], while plant-derived EVs are increasingly explored for their anti-inflammatory properties [19,20].

In contrast, EVs from animal-based medicinal materials, particularly invertebrates, remain poorly characterized. As the source of EVs critically influences their composition, safety, and potential applications, the identification of suitable biological systems and reliable isolation strategies is essential for expanding EV-based research in these underexplored contexts. Although EV secretion has been documented across parasitic helminths, protozoa, and blood-feeding arthropods [21,22], vesicles derived from animal materials used in traditional medicine remain largely unexplored; notably, exosome-like nanoparticles isolated from the medicinal insect Periplaneta americana retained wound-healing activity,

indicating that pharmacologically active vesicles can be recovered from medicinal animal sources [23].

H. nipponia represents a suitable biological system for exploring EVs from animal-derived sources due to its well-developed secretory system and the availability of both secretion-derived and tissue-derived materials [24]. The salivary gland system is characterized by active secretion processes and continuous release of protein-rich components [25], providing a biologically relevant source for investigating EV-enriched preparations. In contrast, tissue-derived samples, such as the leech head, represent a more complex biological matrix that may contain EVs originating from multiple cell types. This dual-source characteristic enables the investigation of EVs across both secretion-based and tissue-derived contexts within the same system. In blood-feeding arthropods, vesicles released into saliva and salivary glands have been shown to deliver immunomodulatory and wound-healing-related cargo to the host skin interface [22,26], which supports the view that secretory organs of hematophagous invertebrates are a productive source of functionally active EVs.

Despite these advantages, it remains unclear whether EVs can be reliably isolated from these biological materials to compare operationally separated EV-enriched fractions and how EV composition varies between sources and vesicle subtypes. In addition, tissue-derived matrices release intracellular and extracellular matrix components upon dissociation, so dedicated enrichment strategies are required to obtain preparations that fulfill current consensus criteria [27,28].

We hypothesized that EV-enriched fractions could be successfully isolated from both fresh salivary gland secretions and lyophilized head tissue of *H. nipponia*, and that the lyophilized tissue retains characteristic EV morphology and a protein profile partially overlapping with that of fresh salivary gland-derived EVs, including bioactive proteins relevant to the medicinal properties of leeches. To test this hypothesis, we aimed to isolate EVs from salivary gland secretions (SGS) and lyophilized head tissue (LP) of *H. nipponia* and to characterize their structural features and molecular composition. By combining morphological characterization and proteomic analysis, this study establishes an experimental framework for EV isolation from invertebrate medicinal materials and enables a comparative assessment of EV composition across different biological sources and vesicle subtypes.

2. Materials and Methods

2.1. Sample Preparation and Isolation of Extracellular Vesicles

H. nipponia specimens were obtained from Liwen Aquaculture Facility (Dalian, Liaoning, China). Live leeches were maintained in a dark-controlled environment at China Jiliang University and housed in transparent culture tanks (with dimensions of 5 L). The animals were kept in freshwater with daily water replacement under controlled temperature conditions (22 ± 2 °C). *H. nipponia* were fasted for one month before the experiment, and six leeches of similar size and weighing about 0.5 g were selected for the experiment.

Extracellular vesicles (EVs) were isolated from both live and freeze-dried materials. For live specimens, salivary glands were dissected following the method described by Zhu et al. [29]. *H. nipponia* were anesthetized by immersion in a 10% (*v*/*v*) ethanol solution for 10 min. Subsequently, surface mucus was gently removed using a sterile cotton swab, and the animals were secured dorsal-side-up on a dissecting foam board with fine insect pins. A midline incision was made along the ventral abdominal wall under a stereomicroscope, and salivary gland tissue was carefully excised following meticulous removal of adjacent connective tissue using ophthalmic scissors (Figure 1).

The isolated tissues were incubated in 6 cm culture dishes containing 10^{-6} mol/L serotonin to stimulate secretion, and salivary gland secretions (SGS) were collected as described by Marshall and Lent [30].

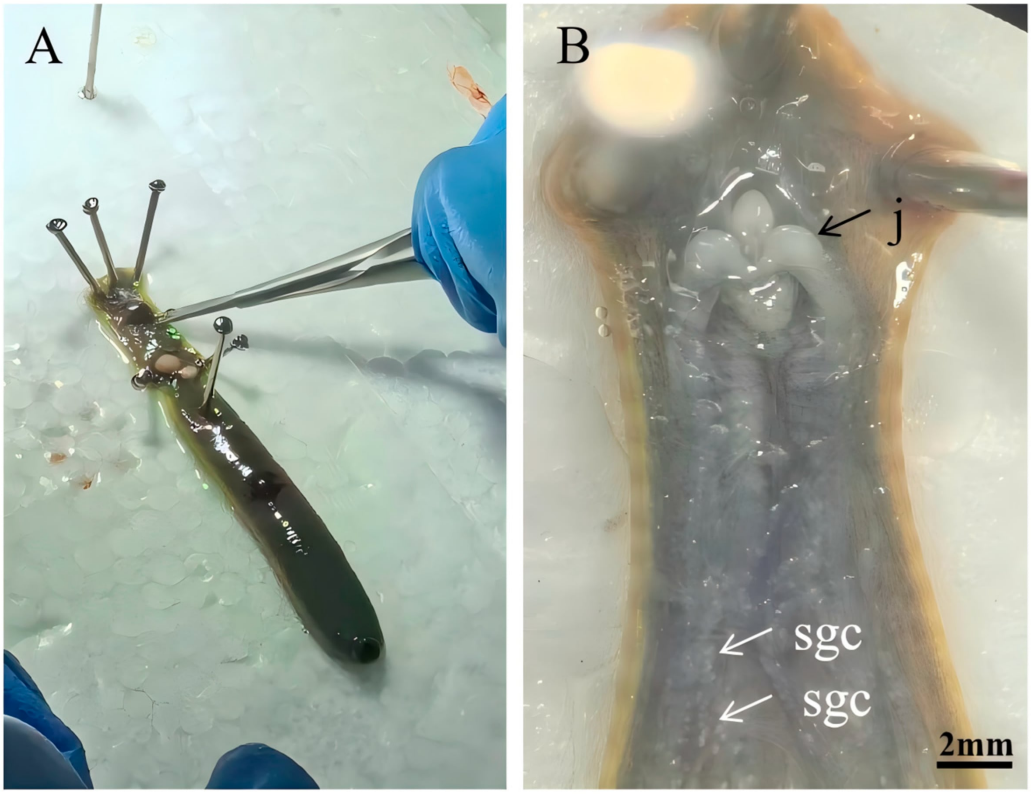


Figure 1. Schematic diagram of the anatomy of *H. nipponia:* (**A**) anatomical locality of the salivary gland tissue of *H. nipponia*; (**B**) salivary gland tissues and jaw structures; j: jaw structures; sgc: Salivary gland cells.

For freeze-dried samples, lyophilized head tissue (LP)was separated and ground into a fine powder. The powder was resuspended in phosphate-buffered saline (PBS) at a ratio of 1 g per 10 mL and left at 4 °C overnight (About 12 h). The supernatant was then collected as the head extract.

EVs were isolated using a differential ultracentrifugation protocol (Figure 2), and two EV-enriched fractions were operationally separated based on centrifugal force: a large-vesicle fraction (hereafter termed MV-enriched fraction) at 10,000× *g*, and a small-vesicle fraction (hereafter termed EXO-enriched fraction) at 130,000× *g*. Briefly, both SGS and LPS were first centrifuged at 300× *g* for 10 min, followed by 3000× *g* and 5000× *g* for 20 min each, to remove cells and large debris. The resulting supernatant was then centrifuged at 10,000× *g* for 45 min to pellet the MV-enriched fraction. Subsequently, the supernatant was further ultracentrifuged at 130,000× *g* for 70 min to obtain the EXO-enriched fraction. All centrifugation steps were performed at 4 °C using an ultracentrifuge (CP100MX, Hitachi, Tokyo, Japan) [31,32].

2.2. Morphological and Size Characterization of Extracellular Vesicles

EV samples were deposited onto 200-mesh copper grids coated with carbon support films and allowed to adsorb for 1 min at room temperature. Excess liquid was carefully removed using filter paper, and the grids were negatively stained with 2% uranyl acetate [33]. After air drying, the samples were examined using a transmission electron microscope (Talos L120C, Thermo Fisher Scientific, Waltham, MA, USA), and representative images were acquired.

For nanoparticle tracking analysis (NTA), the detection was completed by the ZetaView-PMX120-Z (Particle Metrix, Meerbusch, Germany) instrument and its companion software ZetaView (version 8.05). EV samples were diluted in PBS to an appropriate con-

centration prior to measurement. The instrument was calibrated using 100 nm polystyrene bead standards. During acquisition, images were recorded at 11 different positions for each sample and analyzed automatically by the software. The measurement temperature was maintained at approximately 23 °C. Particle size distribution and mean particle diameter were calculated using the instrument software [34–36].

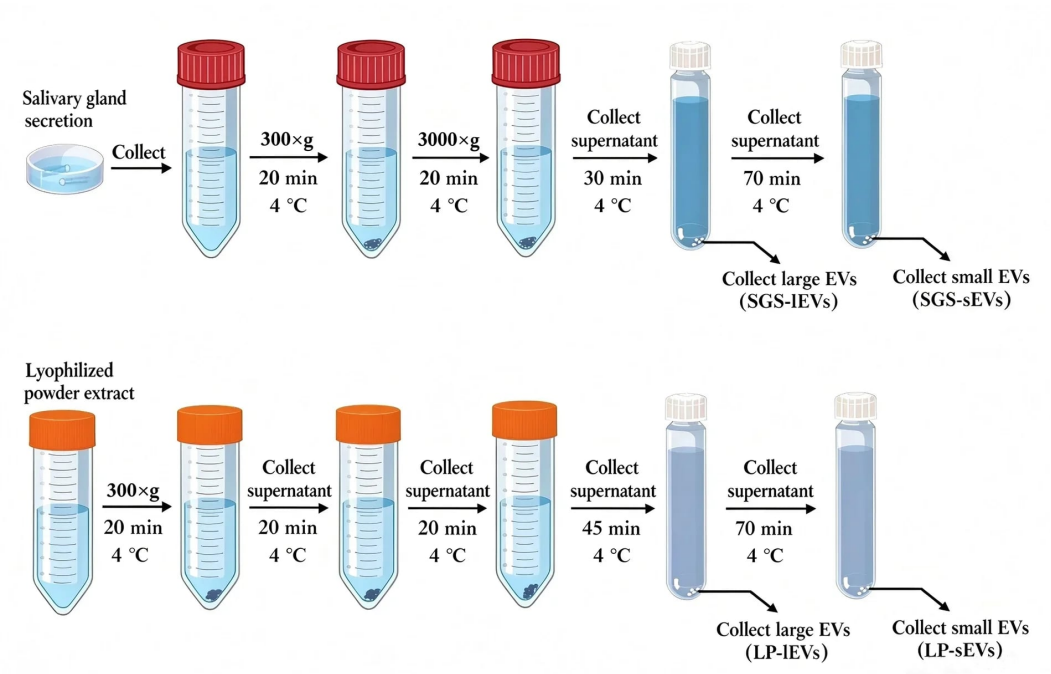


Figure 2. Flow chart of the isolation of four extracellular vesicles by differential ultracentrifugation.

2.3. Proteomic Analysis and Functional Annotation of Extracellular Vesicles

Proteomic analysis of EV samples was performed by Shanghai Applied Protein Technology Co., Ltd. (Shanghai Applied Protein Technology Co., Ltd., Shanghai, China). using data-independent acquisition (DIA) mass spectrometry [37,38]. All analyses were conducted with three independent biological replicates for each group. EV samples were lysed in SDT buffer (4% sodium dodecyl sulfate, 100 mM Tris-HCl, pH 7.6) and boiled for protein denaturation. After centrifugation at 14,000× *g*, the supernatant was collected and protein concentration was determined using the bicinchoninic acid (BCA) assay. A total of 15 µg protein per sample was separated by SDS-PAGE following mixing with loading buffer and heat denaturation, and visualized by Coomassie staining. Proteins were reduced with tris (2-carboxyethyl) phosphine (TCEP) and alkylated with iodoacetamide prior to enzymatic digestion. Samples were digested using trypsin and Lys-C at 37 °C for 3 h.

The resulting peptides were desalted using strong cation exchange solid-phase extraction (SPE MCX cartridges) and concentrated by vacuum centrifugation. Peptides were reconstituted in 0.1% formic acid, quantified by UV absorbance at 280 nm, and spiked with indexed retention time (iRT) peptides (Biognosys, Schlieren, Switzerland) for retention time calibration. Peptide separation was performed using an Evosep One liquid chromatography system (Evosep, Odense, Denmark), and mass spectrometry analysis was conducted on a timsTOF Pro 2 instrument (Bruker Daltonics, Bremen, Germany) in DIA mode. MS1 spectra were acquired over an m/z range of 100–1700 using four acquisition windows with an accumulation time of 100 ms per window. Data were collected using the dia-PASEF acquisition method, with collision energy linearly correlated to the inverse ion mobility (1/K0).

Raw data were processed using Spectronaut software (version 19.7, Biognosys, Switzerland). The protein reference database for mass spectrometry searching was downloaded from the National Center for Biotechnology Information (NCBI Hirudinidae-1414-20230529). A maximum of two missed cleavages was allowed. Carbamidomethylation of cysteine was set as a fixed modification, while oxidation of methionine and protein N-terminal acetylation were set as variable modifications. Protein identifications were accepted at a false discovery rate (FDR) $\leq 1\%$. For differential expression analysis, proteins with a fold change (FC) > 1.5 or <0.67 and p value < 0.05 were considered significantly differentially expressed, and proteins showing more than 10-fold changes were highlighted. Domain enrichment analysis was performed using Fisher's exact test with multiple testing correction. Functional annotation of differentially expressed proteins was conducted using Gene Ontology (GO) analysis (biological process) and Kyoto Encyclopedia of Genes and Genomes (KEGG) pathway analysis, implemented through the OmicsBean platform.

2.4. Statistical Analysis

All statistical analyses were performed using GraphPad Prism 9.0 (GraphPad Software, Boston, MA, USA) and R software (version 4.2.1, R Foundation for Statistical Computing, Vienna, Austria). For particle size comparison between EV-enriched fractions, Student's *t*-test was used for pairwise comparisons. For functional and domain enrichment analysis of proteomic data, Fisher's exact test was applied with multiple testing correction. All experiments were performed with at least three independent biological replicates. A p-value < 0.05 was considered statistically significant.

3. Results

3.1. Morphology, Particle Size and Concentration Characterization of H. nipponia-Derived Extracellular Vesicles

Transmission electron microscopy (TEM) (Figure 3) and nanoparticle tracking analysis (NTA) (Figure 4) showed that all EV samples exhibited typical morphological characteristics consistent with extracellular vesicles. Both MV and EXO populations displayed membrane-bound vesicular structures with sizes within the expected nanoscale range. SGS-lEVs exhibited irregular spherical or ellipsoidal morphology, with an average particle diameter of 228.0 ± 122.9 nm. In comparison, LP-lEVs were generally spherical or near-spherical and showed a smaller average diameter of 193.3 ± 82.5 nm. Both SGS-sEVs and LP-sEVs displayed typical cup-shaped morphology with intact membrane structures. The average particle diameters of SGS-sEVs and LP-sEVs were 191.2 ± 77.7 nm and 182.1 ± 60.4 nm, respectively, with relatively narrower size distributions compared to lEVs.

Proteomic characterization of EV-enriched fractions: A total of 3340 proteins and 20,351 peptides were identified across all EV samples, indicating successful protein extraction and detection. Among these, 1171 proteins were shared across all four EV populations, representing proteins shared across all four preparations. These shared proteins were primarily associated with fundamental cellular functions, including protein folding, energy metabolism, cytoskeleton organization, and signal transduction (Figure 5).

In addition, several proteins with reported pharmacological activities were identified [39–41], including Saratin, Theromyzin, Hyaluronidase, Hirudin, Destabilase I, and Eglin C. Among these, Saratin, Theromyzin, and Hyaluronidase were detected in all EV populations, whereas Hirudin, Destabilase I, and Eglin C were detected only in SGS-derived EVs.

Six proteins with potential pharmacological activity were screened from all identified proteins, and their distribution characteristics in the four types of EVs are shown in Table 1. These proteins are involved in functions such as anticoagulation, antithrombosis, anti-inflammation, antibiosis, and extracellular matrix degradation, and exhibit differen-

tial distribution among the four types of EVs. Among them, Saratin, Theromyzin and Hyaluronidase were all identified in the four types of EVs, while Hirudin, Destabilase I and Eglin C were only detected in SGS-derived EVs (SGS-lEVs, SGS-sEVs).

Table 1. Distribution Characteristics of Key Active Proteins in Extracellular Vesicles from Salivary Glands of Hirudo nipponica.

Protein ID	Protein	SGS-lEVs	SGS-sEVs	LP-lEVs	LP-sEVs
QDZ37419.1	Hirudin	√	√		
AAA96144.1	Destabilase I	√	√		
P01051.1	Eglin C	√	√		
Q6T6C1	Theromyzin	√	√	√	√
WBW88639.1	Saratin	√	√	√	√
AHV78514.1	Hyaluronidase	√	√	√	√

√: protein identified in the corresponding EV-enriched fraction.

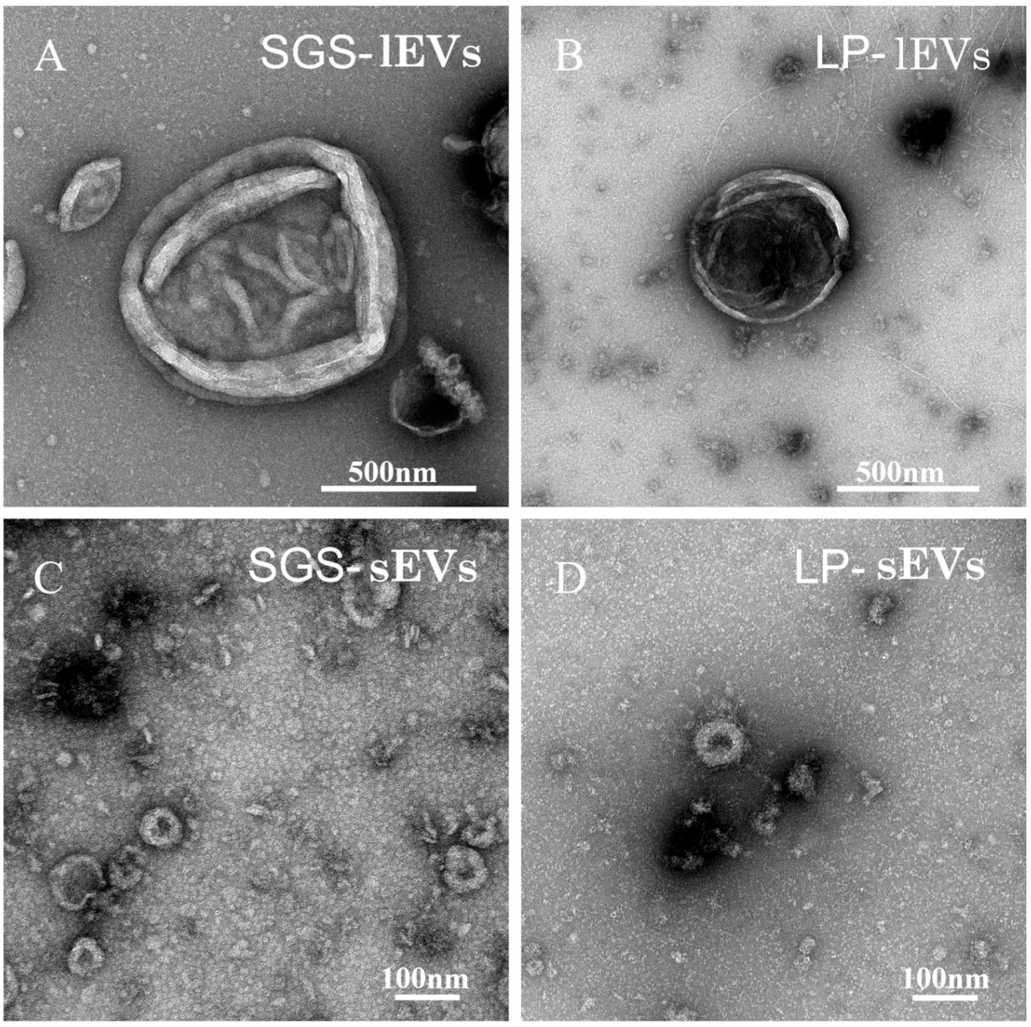


Figure 3. Morphology of four types of extracellular vesicles from the salivary glands of Hirudo nipponica under transmission electron microscope. (**A**) Morphological diagram of salivary gland lEVs; (**B**) morphological diagram of lEVs in extract of lyophilized powder of head; (**C**) morphological diagram of sEVs in salivary gland secretion; (**D**) morphological diagram of sEVs extracted from lyophilized powder of head.

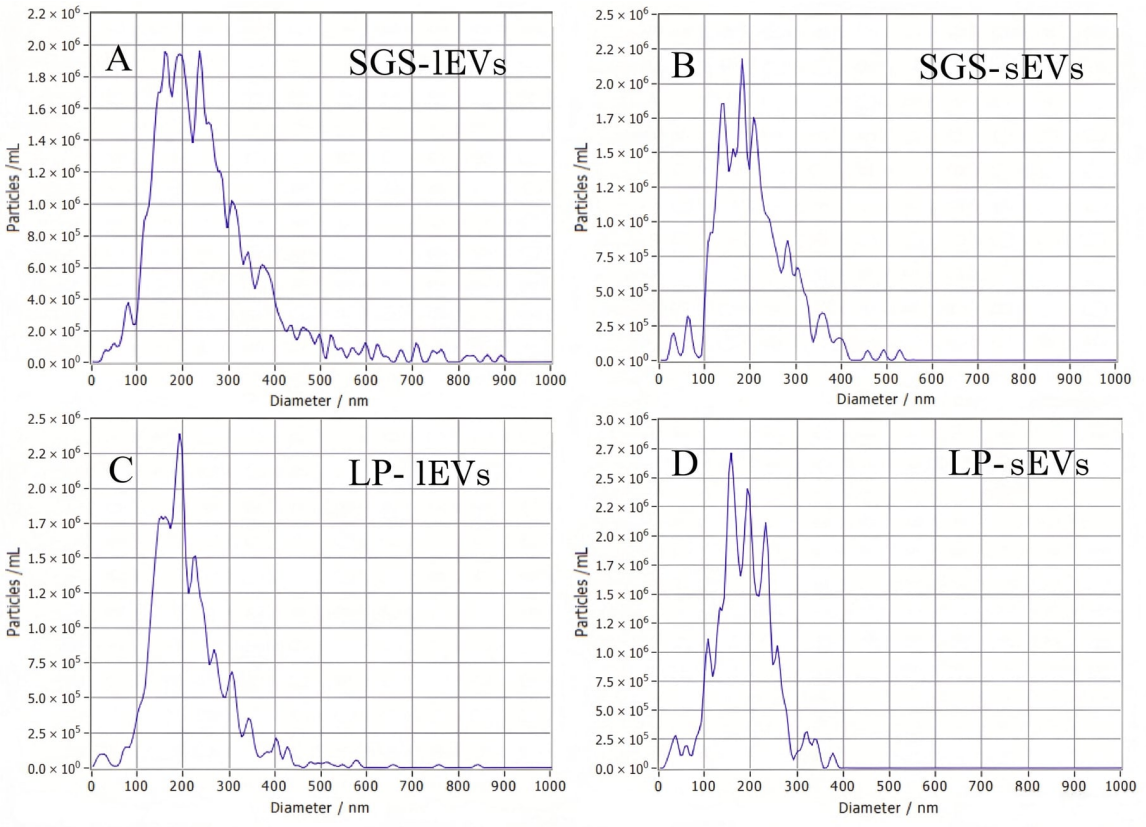


Figure 4. Particle size distribution curves of four kinds of extracellular vesicles in the salivary gland of Hirudo nipponica. (**A**) Size distribution of salivary gland secretory large extracellular vesicles (SGS-lEVs); (**B**) size distribution curve of small extracellular vesicles derived from salivary gland secretion (SGS-sEVs); (**C**) particle size distribution curve of large extracellular vesicles (LP-lEVs) in lyophilized powder extract of head; (**D**) particle size distribution curve of small extracellular vesicles extracted from lyophilized head powder (LP-sEVs).

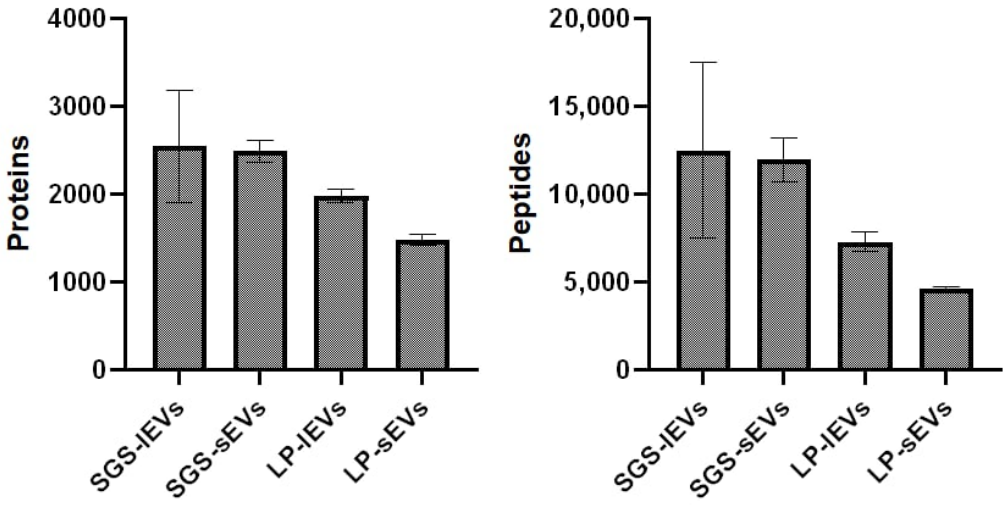


Figure 5. Number of identified proteins and peptides in four types of extracellular vesicles from Hirudo nipponica.

3.2. Proteomic Differences Between SGS- and LP-Derived EVs

Differential expression analysis identified 561 proteins between SGS-lEVs and LP-lEVs, including 267 upregulated and 294 downregulated proteins. Among these, 16 proteins were highly upregulated and 38 were highly downregulated. In the EXO populations, 669 differ-

entially expressed proteins were identified between SGS-sEVs and LP-sEVs, including 219 upregulated and 450 downregulated proteins, with 15 highly upregulated and 37 highly downregulated proteins (Figure 6).

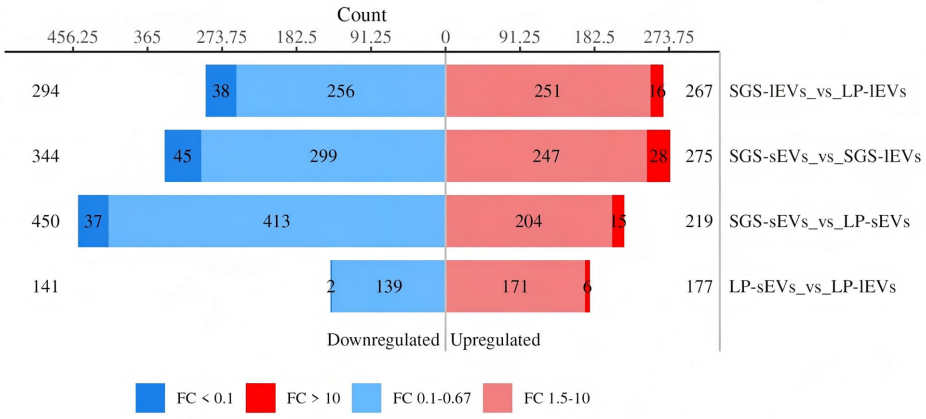


Figure 6. Bar chart of protein quantification differential results.

Domain enrichment analysis showed that proteins differing between SGS-lEVs and LP-lEVs were primarily associated with ion binding and signal transduction, lipid and carbohydrate metabolism, protein interaction, and membrane trafficking. In SGS-sEVs versus LP-sEVs, enriched domains were mainly related to protease regulation, vesicle transport, calcium signaling, and extracellular matrix remodeling (Figure 7A,C).

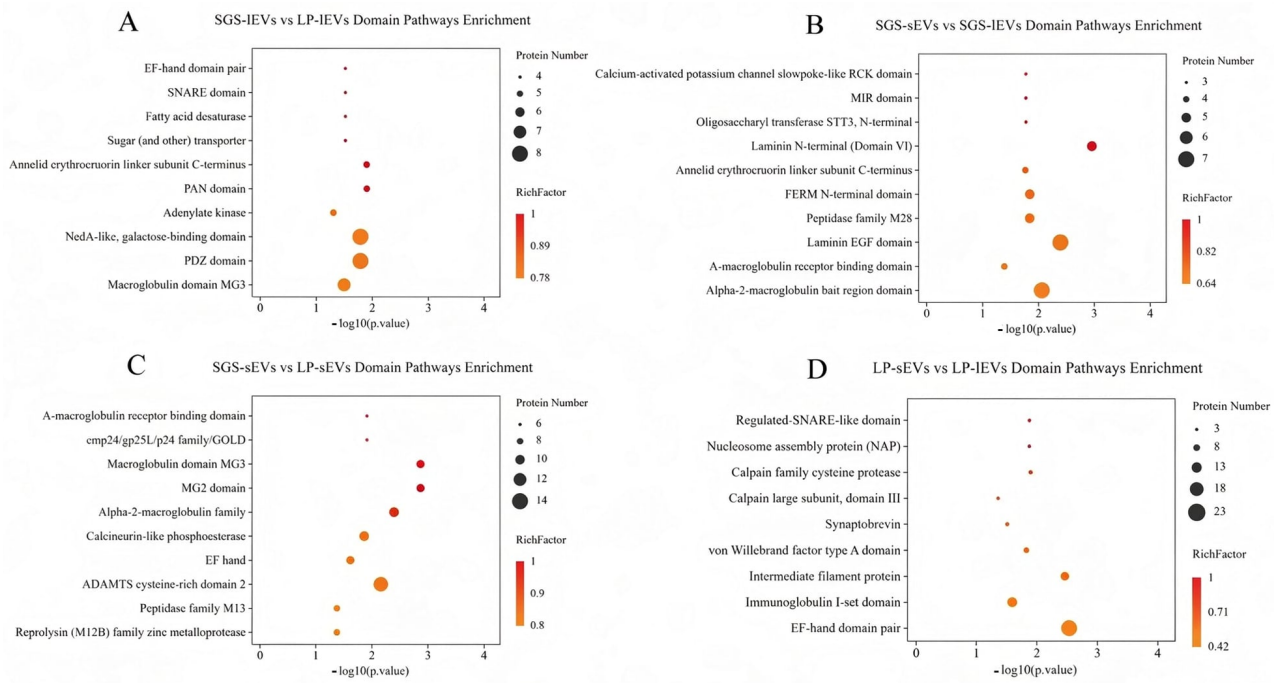


Figure 7. Bubble plots of domain enrichment analysis for each comparison group. (**A**) Domain enrichment analysis comparing SGS-lEV and LP-lEV groups; (**B**) domain enrichment analysis comparing SGS-sEV and SGS-lEV groups; (**C**) domain enrichment analysis comparing SGS-sEV and LP-sEV groups; (**D**) domain enrichment analysis comparing LP-sEV and LP-lEV groups. The horizontal axis displays the *p*-value (converted to $-\log_{10}$) calculated using Fisher's exact test; a higher value indicates a greater statistical significance of enrichment in the corresponding domain category. The vertical axis lists domain names, where the size of each bubble represents the number of differentially expressed proteins, and the color indicates the Rich Factor, where colors closer to red correspond to higher Rich Factor values.

GO and KEGG enrichment analyses indicated that differentially expressed proteins between SGS-lEVs and LP-lEVs were mainly involved in metabolic processes, transmembrane transport, and signaling pathways. In contrast, proteins differing between SGS-sEVs and LP-sEVs were associated with immune-related processes, protein turnover, extracellular matrix interactions, and signal transduction pathways (Figures 8A,C and 9A,C).

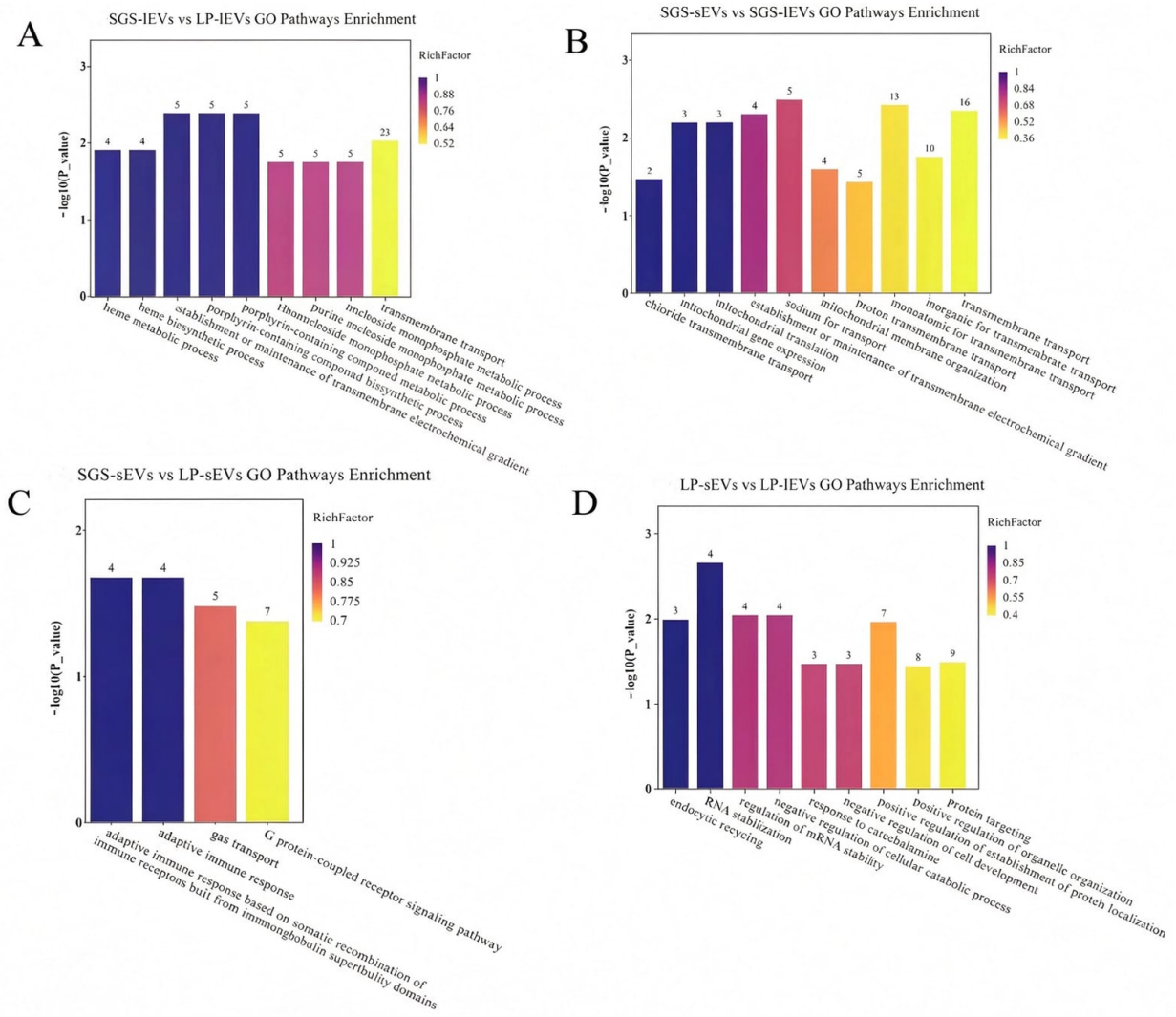


Figure 8. GO functional enrichment bar plots of differentially expressed proteins across all comparison groups (BP). (**A**) GO functional enrichment analysis for the SGS-lEV vs. LP-lEV groups; (**B**) GO functional enrichment analysis for the SGS-sEV vs. SGS-lEV groups; (**C**) GO functional enrichment analysis for the SGS-sEV vs. LP-sEV groups; (**D**) GO functional enrichment analysis for the LP-sEV vs. LP-lEV groups. The horizontal axis displays GO functional annotation names, with color indicating the enrichment degree (Rich Factor)—the closer the color to blue, the greater the Rich Factor value; the number above each bar indicates the number of differentially expressed proteins contained in that GO functional annotation; the vertical axis shows the *p*-value (converted to $-\log_{10}$) calculated using Fisher's exact test, reflecting the statistical significance of the enrichment.

Upregulated: proteins with upregulated differential expression; downregulated: proteins with downregulated expression.

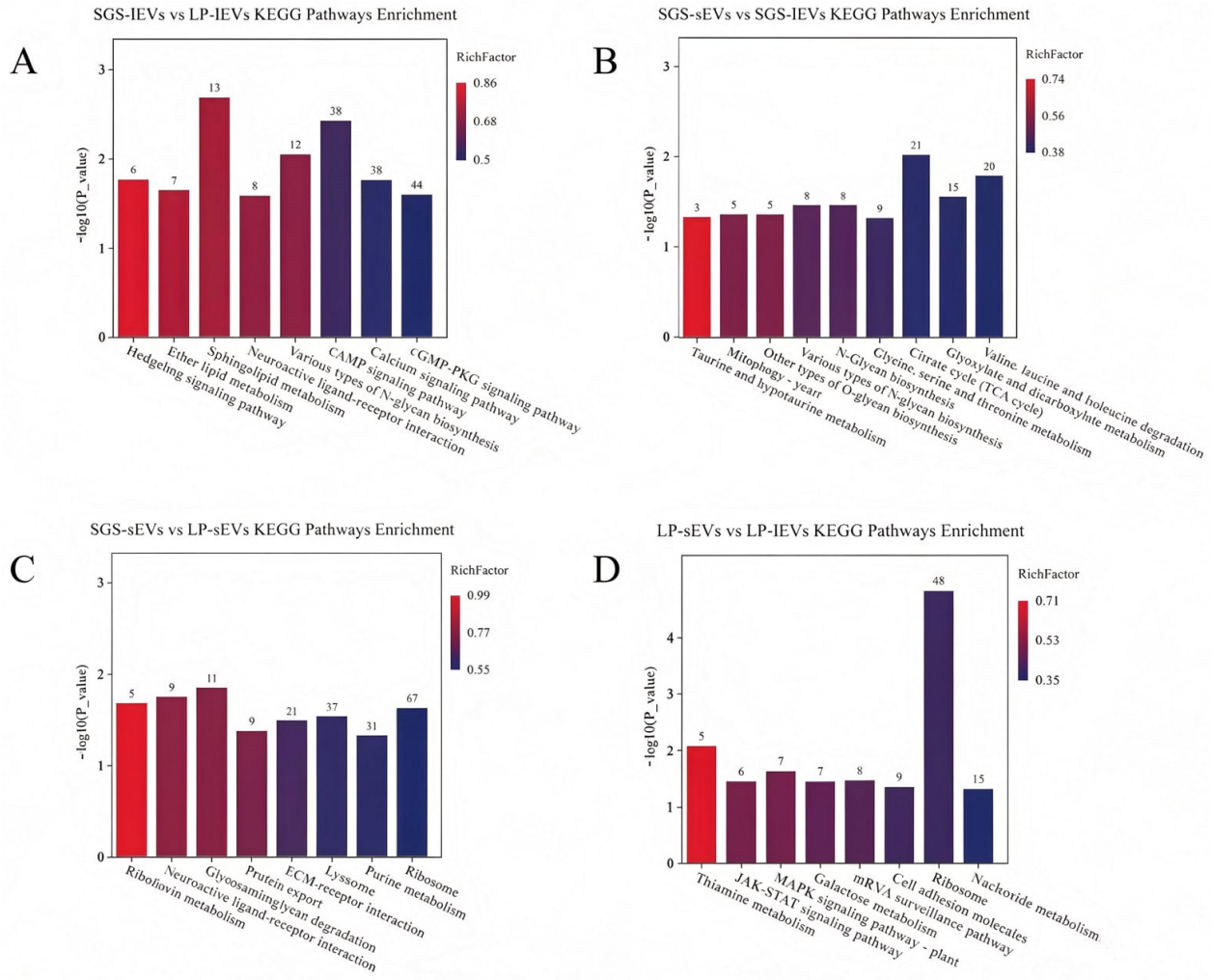


Figure 9. KEGG pathway enrichment bar plots of differentially expressed proteins across all comparison groups. (**A**) KEGG pathway enrichment analysis for the SGS-lEV vs. LP-lEV groups; (**B**) KEGG pathway enrichment analysis for the SGS-sEV vs. SGS-lEV groups; (**C**) KEGG pathway enrichment analysis for the SGS-sEV vs. LP-sEV groups; (**D**) KEGG pathway enrichment analysis for the LP-sEV vs. LP-lEV groups. The horizontal axis displays the names of KEGG pathways, with colors indicating the enrichment degree (Rich Factor)—the closer the color to red, the greater the Rich Factor value. The number above each bar indicates the number of differentially expressed proteins contained in that pathway. The vertical axis shows the *p*-values (converted to $-\log_{10}$) calculated using Fisher's exact test, reflecting the statistical significance of the enrichment results.

3.3. Proteomic Differences Between EV Subtypes (lEVs vs. sEVs)

Differential expression analysis identified 619 proteins between SGS-sEVs and SGS-lEVs, including 275 upregulated and 344 downregulated proteins. Among these, 28 proteins were highly upregulated and 45 were highly downregulated. In LP-derived EVs, 318 differentially expressed proteins were identified between LP-sEVs and LP-lEVs, including 177 upregulated and 141 downregulated proteins, with 6 highly upregulated and 2 highly downregulated proteins (Figure 6).

Domain enrichment analysis showed that proteins differing between SGS-sEVs and SGS-lEVs were mainly associated with extracellular matrix organization, protease regulation, protein interaction, ion transport, and glycosylation-related functions. In LP-derived EVs, enriched domains between sEVs and lEVs were related to membrane trafficking, cytoskeleton organization, calcium signaling, protease activity, and immune recognition (Figure 7B,D).

GO and KEGG enrichment analyses indicated that proteins differing between SGS-sEVs and SGS-lEVs were mainly involved in ion transport, mitochondrial function, metabolic pathways, and glycosylation processes. In LP-derived EVs, enriched functions included RNA regulation, intracellular trafficking, cell signaling, and metabolic pathways (Figures 8B,D and 9B,D).

4. Discussion

This study provides a systematic characterization of extracellular vesicles (EVs) derived from *H. nipponia*. EVs were successfully isolated from both salivary gland secretions and head-derived materials, and distinct vesicle subtypes were obtained. Proteomic analysis further revealed variations in EV composition associated with both tissue origin and vesicle subtype.

This study identified several proteins with documented pharmacological activities—including hirudin, destabilase I, eglins C, saratin, theromyzin, and hyaluronidase—in extracellular vesicles (EVs) isolated from four leech salivary gland samples. These proteins are well-established bioactive constituents of leech saliva [42,43]. The findings corroborate that EVs serve as carriers for functionally relevant molecules—particularly anticoagulant, antithrombotic, and anti-inflammatory agents—secreted by salivary gland cells. Whether these proteins are encapsulated within EVs or merely associated with the vesicle surface remains to be determined, as does whether EV association influences their stability or biological activity. These findings provide a proteomic basis for further functional investigation of EV-associated bioactive molecules from leech salivary glands [44–47].

Saratin, theromycin, and hyaluronidase were consistently identified across all four extracellular vesicle (EV) preparations. Saratin exhibits potent antiplatelet activity by inhibiting both platelet adhesion and aggregation, thereby suppressing thrombus formation [48,49]. Theromycin is an anionic antimicrobial peptide demonstrating robust antibacterial efficacy specifically against Gram-positive bacteria [50]. Hyaluronidase catalyzes the hydrolysis of hyaluronic acid in the extracellular matrix, compromising structural integrity of host tissue barriers and facilitating enhanced diffusion and tissue penetration of bioactive salivary components from leeches [51,52]. Collectively, these findings suggest that the EVs serve as natural carriers for salivary-gland-derived bioactive molecules and possess multifunctional therapeutic potential—including antithrombotic, antimicrobial, and extracellular matrix–modulating activities. Moreover, Hirudin, Destabilase I, and Eglin C were exclusively detected in EVs isolated from freshly collected leech salivary gland secretions (SGS), whereas they were undetectable in EVs derived from lyophilized leech powder (LP). These proteins were detected in SGS-derived EV preparations but not detected in the LP-derived preparations under the present proteomic conditions. In contrast, SGS-derived EVs are obtained directly from the physiologically active secretion of leech salivary glands. The protein composition of SGS-derived preparations reflects the dissected and 5-HT-stimulated salivary gland secretion. Functionally, these three proteins act at distinct steps within the coagulation and inflammatory cascades: Hirudin—recognized as the most potent and specific thrombin inhibitor identified to date—irreversibly inhibits thrombin, thereby blocking the final common pathway of both intrinsic and extrinsic coagulation and serving as the principal mediator of anticoagulant activity [53–56]. Destabilase I exerts thrombolytic effects via enzymatic degradation of cross-linked fibrin and demonstrates broad-spectrum antibacterial activity through both enzymatic and non-enzymatic mechanisms [57–59]. Eglin C, a serine protease inhibitor, suppresses inflammation-associated proteases—including neutrophil elastase and cathepsin G—thereby attenuating inflammatory responses [60,61]. Collectively, these findings indicate that SGS-derived EV preparations contained a broader detectable

profile of proteins with reported anticoagulant, thrombolytic, and anti-inflammatory activities compared with LP-derived preparations.

In recent years, extracellular vesicles derived from medicinal animals have attracted increasing attention as naturally derived bioactive carriers. EV-enriched fractions from other medically relevant invertebrates—such as the medicinal earthworm *Eisenia fetida*, medicinal snail mucus, and other leech species—have been reported to carry anti-inflammatory, pro-repair and immunomodulatory protein cargo, with particle sizes mostly ranging from 50 to 300 nm [62]. Compared with these reported medicinal animal EVs, the EV-enriched fractions from *H. nipponia* in this study show a comparable size distribution and share conserved EV marker proteins, while also harboring unique protein families closely associated with the classic pharmacological activities of leeches, including anticoagulant, anti-inflammatory and matrix-regulatory molecules [63]. In particular, the successful isolation of EVs from lyophilized head tissue provides a more convenient, storable sample form for developing leech-derived bioactive materials, which is favorable for long-term preservation and large-scale preparation [64]. Although these proteomic features suggest promising therapeutic potential of *H. nipponia* EVs, their actual biological activities and safety profiles still require systematic functional validation through in vitro and in vivo studies before further translational application.

Collectively, our morphological and proteomic data support the proposed hypothesis. Typical EV structures and characteristic protein markers were identified in both fresh salivary gland and lyophilized head-derived fractions, confirming that lyophilization preserves the major EV populations and their core protein cargo. However, the exact biological functions of these EV-associated proteins remain to be functionally validated in subsequent studies.

This study has several limitations that should be acknowledged. First, the current work is limited to morphological characterization and proteomic profiling of EV-enriched fractions from *H. nipponia*, and no in vitro functional assays have been performed to verify the biological activities of these EVs and their protein cargo. Second, the EV preparations in this study were obtained via differential ultracentrifugation, which yields operationally defined EV-enriched fractions rather than pure populations of specific EV subtypes with confirmed biogenesis. Third, only two sample sources (fresh salivary gland secretions and lyophilized head tissue) were included, and the characteristics of EVs from other tissues or physiological states of leeches remain to be explored. Further functional validation and more refined isolation strategies will be carried out in our follow-up research.

5. Conclusions

This study successfully isolated and characterized extracellular vesicles (EVs) from H. nipponia and systematically analyzed the proteomic profiles of lEVs and sEVs derived from salivary gland secretions (SGS) and lyophilized head powder (LP). Proteomic analysis revealed that the 1171 core proteins shared by the four EV subsets primarily sustain the fundamental biological functions of EVs, whereas subset-specific proteins reflect heterogeneity in biogenesis and protein sorting across different EV subtypes. A range of pharmacologically active proteins, represented by Hirudin, Destabilase I, and Eglin C, were successfully identified, confirming that EVs serve as critical functional carriers for the transport of bioactive substances in leeches.

Comparative analyses further demonstrated that SGS-derived EVs exhibit a more intact pharmacological component profile compared to those isolated from the traditional LP source, suggesting that research directly targeting the salivary gland secretory system more closely aligns with the physiological and pharmacological essence of leech bioactivity. Overall, the present study reveals proteomic differences among source- and centrifugation-

defined EV-enriched fractions. SGS-derived preparations exhibited a broader detectable profile of pharmacologically relevant proteins than LP-derived preparations.

Author Contributions: Conceptualization, M.-X.J. and X.Q.; Methodology, M.-X.J., Y.-L.Z. and X.Q.; Formal analysis, M.-X.J. and Y.-L.Z.; Investigation, M.-X.J.; Resources, Y.-Y.L.; Data curation, Q.L. and W.-M.W.; Writing—original draft, M.-X.J. and Y.-L.Z.; Writing—review & editing, Y.-L.Z., X.Q., Q.L. and Y.-Y.L.; Visualization, W.-M.W.; Supervision, X.Q., Q.L., W.-M.W. and Y.-Y.L.; Project administration, Y.-Y.L.; Funding acquisition, Y.-Y.L. All authors have read and agreed to the published version of the manuscript.

Funding: This research was funded by the China Jiliang University Science and Technology Cooperation Project, grant number 03106–231601 (to Yuan-Yuan Luo).

Informed Consent Statement: Not applicable.

Data Availability Statement: The mass spectrometry proteomics data have been deposited in the ProteomeXchange Consortium via the PRIDE [1] partner repository with the dataset identifier PXD087321 and 10.6019/PXD087321.

Acknowledgments: We thank Yuchen Zhang in the Center of Cryo-Electron Microscopy (CCEM), Zhejiang University for her technical assistance on Thermo Scientific Talos L120C Electron Microscopy.

Conflicts of Interest: The authors declare no conflicts of interest.

References

1. Raposo, G.; Stoorvogel, W. Extracellular vesicles: Exosomes, microvesicles, and friends. *J. Cell Biol.* **2013**, *200*, 373–383. [CrossRef] [PubMed]
2. Kalluri, R.; LeBleu, V.S. The biology, function, and biomedical applications of exosomes. *Science* **2020**, *367*, eaau6977. [CrossRef] [PubMed]
3. El Andaloussi, S.; Mäger, I.; Breakefield, X.O.; Wood, M.J.A. Extracellular vesicles: Biology and emerging therapeutic opportunities. *Nat. Rev. Drug Discov.* **2013**, *12*, 347–357. [CrossRef] [PubMed]
4. Van Niel, G.; D'Angelo, G.; Raposo, G. Shedding light on the cell biology of extracellular vesicles. *Nat. Rev. Mol. Cell Biol.* **2018**, *19*, 213–228. [CrossRef] [PubMed]
5. Colombo, M.; Raposo, G.; Théry, C. Biogenesis, secretion, and intercellular interactions of exosomes and other extracellular vesicles. *Annu. Rev. Cell Dev. Biol.* **2014**, *30*, 255–289. [CrossRef] [PubMed]
6. Welsh, J.A.; Goberdhan, D.C.I.; O'Driscoll, L.; Buzas, E.I.; Blenkiron, C.; Bussolati, B.; Cai, H.; Di Vizio, D.; Driedonks, T.A.P.; Erdbrügger, U.; et al. Minimal information for studies of extracellular vesicles (MISEV2023): From basic to advanced approaches. *J. Extracell. Vesicles* **2024**, *13*, e12404. [CrossRef] [PubMed]
7. Jeppesen, D.K.; Zhang, Q.; Coffey, R.J. Extracellular vesicles and nanoparticles at a glance. *J. Cell Sci.* **2024**, *137*, jcs260201. [CrossRef] [PubMed]
8. Thery, C.; Clayton, A.; Amigorena, S.; Raposo, G. Isolation and characterization of exosomes from cell culture supernatants and biological fluids. *Curr. Protoc. Cell Biol.* **2006**, *3*, 3.22.1–3.22.29. [CrossRef] [PubMed]
9. Théry, C.; Witwer, K.W.; Aikawa, E.; Alcaraz, M.J.; Anderson, J.D.; Andriantsitohaina, R.; Antoniou, A.; Arab, T.; Archer, F.; Atkin-Smith, G.K.; et al. Minimal information for studies of extracellular vesicles 2018 (MISEV2018): A position statement of the International Society for Extracellular Vesicles and update of the MISEV2014 guidelines. *J. Extracell. Vesicles* **2018**, *7*, 1535750. [CrossRef] [PubMed]
10. Lötvall, J.; Hill, A.F.; Hochberg, F.; Buzás, E.I.; Di Vizio, D.; Gardiner, C.; Gho, Y.S.; Kurochkin, I.V.; Mathivanan, S.; Quesenberry, P.; et al. Minimal experimental requirements for definition of extracellular vesicles and their functions: A position statement from the International Society for Extracellular Vesicles. *J. Extracell. Vesicles* **2014**, *3*, 26913. [CrossRef] [PubMed]
11. Witwer, K.W.; Théry, C. Extracellular vesicles or exosomes? On primacy, precision, and popularity influencing a choice of nomenclature. *J. Extracell. Vesicles* **2019**, *8*, 1648167. [CrossRef] [PubMed]
12. Herrmann, I.K.; Wood, M.J.A.; Fuhrmann, G. Extracellular vesicles as a next-generation drug delivery platform. *Nat. Nanotechnol.* **2021**, *16*, 748–759. [CrossRef] [PubMed]
13. Elsharkasy, O.M.; Nordin, J.Z.; Hagey, D.W.; De Jong, O.G.; Schiffelers, R.M.; Andaloussi, S.E.; Vader, P. Extracellular vesicles as drug delivery systems: Why and how? *Adv. Drug Deliv. Rev.* **2020**, *159*, 332–343. [CrossRef] [PubMed]
14. Gardiner, C.; Di Vizio, D.; Sahoo, S.; Théry, C.; Witwer, K.W.; Wauben, M.; Hill, A.F. Techniques used for the isolation and characterization of extracellular vesicles: Results of a worldwide survey. *J. Extracell. Vesicles* **2016**, *5*, 32945. [CrossRef] [PubMed]

15. Van Deun, J.; Mestdagh, P.; Sormunen, R.; Cocquyt, V.; Vermaelen, K.; Vandesompele, J.; Bracke, M.; De Wever, O.; Hendrix, A. The impact of disparate isolation methods for extracellular vesicles on downstream RNA profiling. *J. Extracell. Vesicles* **2014**, *3*, 24858. [CrossRef] [PubMed]
16. Böing, A.N.; van der Pol, E.; Grootemaat, A.E.; Coumans, F.A.W.; Sturk, A.; Nieuwland, R. Single-step isolation of extracellular vesicles by size-exclusion chromatography. *J. Extracell. Vesicles* **2014**, *3*, 23430. [CrossRef] [PubMed]
17. Kou, M.; Huang, L.; Yang, J.; Chiang, Z.; Chen, S.; Liu, J.; Guo, L.; Zhang, X.; Zhou, X.; Xu, X.; et al. Mesenchymal stem cell-derived extracellular vesicles for immunomodulation and regeneration: A next generation therapeutic tool? *Cell Death Dis.* **2022**, *13*, 580. [CrossRef] [PubMed]
18. Zhang, Y.; Pan, Y.; Liu, Y.; Li, X.; Tang, L.; Duan, M.; Li, J.; Zhang, G. Exosomes derived from human umbilical cord blood mesenchymal stem cells stimulate regenerative wound healing via transforming growth factor-β receptor inhibition. *Stem Cell Res. Ther.* **2021**, *12*, 434. [CrossRef] [PubMed]
19. Teng, Y.; Ren, Y.; Sayed, M.; Hu, X.; Lei, C.; Kumar, A.; Hutchins, E.; Mu, J.; Deng, Z.; Luo, C.; et al. Plant-Derived Exosomal MicroRNAs Shape the Gut Microbiota. *Cell Host Microbe* **2018**, *24*, 637–652.e8. [CrossRef] [PubMed]
20. Dad, H.A.; Gu, T.-W.; Zhu, A.-Q.; Huang, L.-Q.; Peng, L.-H. Plant Exosome-like Nanovesicles: Emerging Therapeutics and Drug Delivery Nanoplatforms. *Mol. Ther.* **2021**, *29*, 13–31. [CrossRef] [PubMed]
21. Coakley, G.; Maizels, R.M.; Buck, A.H. Exosomes and Other Extracellular Vesicles: The New Communicators in Parasite Infections. *Trends Parasitol.* **2015**, *31*, 477–489. [CrossRef] [PubMed]
22. Zhou, W.; Tahir, F.; Wang, J.C.-Y.; Woodson, M.; Sherman, M.B.; Karim, S.; Neelakanta, G.; Sultana, H. Discovery of Exosomes From Tick Saliva and Salivary Glands Reveals Therapeutic Roles for CXCL12 and IL-8 in Wound Healing at the Tick–Human Skin Interface. *Front. Cell Dev. Biol.* **2020**, *8*, 554. [CrossRef] [PubMed]
23. Liao, Q.; Su, L.; Pang, L.; Li, J.; Li, H.; Li, J.; Liu, Y.; Zhang, J. Natural exosome-like nanoparticles derived from ancient medicinal insect Periplaneta americana L. as a novel diabetic wound healing accelerator. *J. Nanobiotechnology* **2023**, *21*, 169. [CrossRef] [PubMed]
24. Dong, H.; Ren, J.-X.; Wang, J.-J.; Ding, L.-S.; Zhao, J.-J.; Liu, S.-Y.; Gao, H.-M. Chinese Medicinal Leech: Ethnopharmacology, Phytochemistry, and Pharmacological Activities. *Evid.-Based Complement. Altern. Med.* **2016**, *2016*, 7895935. [CrossRef] [PubMed]
25. Lu, Z.; Shi, P.; You, H.; Liu, Y.; Chen, S. Transcriptomic analysis of the salivary gland of medicinal leech Hirudo nipponia. *PLoS ONE* **2018**, *13*, e0205875. [CrossRef] [PubMed]
26. Chávez, A.S.O.; Wang, X.; Marnin, L.; Archer, N.K.; Hammond, H.L.; Carroll, E.E.M.; Shaw, D.K.; Tully, B.G.; Buskirk, A.D.; Ford, S.L.; et al. Tick extracellular vesicles enable arthropod feeding and promote distinct outcomes of bacterial infection. *Nat. Commun.* **2021**, *12*, 3696. [CrossRef] [PubMed]
27. White, R.; Sotillo, J.; Ancarola, M.E.; Borup, A.; Boysen, A.T.; Brindley, P.J.; Buzás, E.I.; Cavallero, S.; Chaiyadet, S.; Chalmers, I.W.; et al. Special considerations for studies of extracellular vesicles from parasitic helminths: A community-led roadmap to increase rigour and reproducibility. *J. Extracell. Vesicles* **2023**, *12*, e12298. [CrossRef] [PubMed]
28. Vella, L.J.; Scicluna, B.J.; Cheng, L.; Bawden, E.G.; Masters, C.L.; Ang, C.; Willamson, N.; McLean, C.; Barnham, K.J.; Hill, A.F. A rigorous method to enrich for exosomes from brain tissue. *J. Extracell. Vesicles* **2017**, *6*, 1348885. [CrossRef] [PubMed]
29. Zhu, Y.-L.; Jia, M.-X.; Qu, R.-Y.; Li, Q.; Qiu, X.; Zhao, W.-C.; Luo, Y.-Y. The unique biogenesis pathway of extracellular vesicles in Hirudo nipponia salivary gland cells. *Tissue Cell* **2025**, *99*, 103296. [CrossRef] [PubMed]
30. Marshall, C.G.; Lent, C.M. Excitability and Secretory Activity in the Salivary Gland Cells of Jawed Leeches (Hirudinea: Gnathobdellida). *J. Exp. Biol.* **1988**, *137*, 89–105. [CrossRef] [PubMed]
31. Baranyai, T.; Herczeg, K.; Onódi, Z.; Voszka, I.; Módos, K.; Marton, N.; Nagy, G.; Mäger, I.; Wood, M.J.; El Andaloussi, S.; et al. Isolation of Exo-somes from Blood Plasma: Qualitative and Quantitative Comparison of Ultracentrifugation and Size Exclusion Chromatog-raphy Methods. *PLoS ONE* **2015**, *10*, e0145686. [CrossRef] [PubMed]
32. Nordin, J.Z.; Lee, Y.; Vader, P.; Mäger, I.; Johansson, H.J.; Heusermann, W.; Wiklander, O.P.B.; Hällbrink, M.; Seow, Y.; Bultema, J.J.; et al. Ultrafiltration with size-exclusion liquid chromatography for high yield isolation of extracellular vesicles preserving intact biophysical and functional properties. *Nanomed. Nanotechnol. Biol. Med.* **2015**, *11*, 879–883. [CrossRef] [PubMed]
33. Jung, M.K.; Mun, J.Y. Sample Preparation and Imaging of Exosomes by Transmission Electron Microscopy. *J. Vis. Exp.* **2018**, 56482. [CrossRef] [PubMed] [PubMed Central]
34. Dragovic, R.A.; Gardiner, C.; Brooks, A.S.; Tannetta, D.S.; Ferguson, D.J.P.; Hole, P.; Carr, B.; Redman, C.W.G.; Harris, A.L.; Dobson, P.J.; et al. Sizing and phenotyping of cellular vesicles using Nanoparticle Tracking Analysis. *Nanomed. Nanotechnol. Biol. Med.* **2011**, *7*, 780–788. [CrossRef] [PubMed]
35. Gardiner, C.; Ferreira, Y.J.; Dragovic, R.A.; Redman, C.W.G.; Sargent, I.L. Extracellular vesicle sizing and enumeration by nanoparticle tracking analysis. *J. Extracell. Vesicles* **2013**, *2*, 19671. [CrossRef] [PubMed]
36. Szatanek, R.; Baj-Krzyworzeka, M.; Zimoch, J.; Lekka, M.; Siedlar, M.; Baran, J. The Methods of Choice for Extracellular Vesicles (EVs) Characterization. *Int. J. Mol. Sci.* **2017**, *18*, 1153. [CrossRef] [PubMed]

37. Krasny, L.; Huang, P.H. Data-independent acquisition mass spectrometry (DIA-MS) for proteomic applications in oncology. *Mol. Omics* **2020**, *17*, 29–42. [CrossRef] [PubMed]
38. Fröhlich, K.; Fahrner, M.; Brombacher, E.; Seredynska, A.; Maldacker, M.; Kreutz, C.; Schmidt, A.; Schilling, O. Data-Independent Acquisition: A Milestone and Prospect in Clinical Mass Spectrometry–Based Proteomics. *Mol. Cell. Proteom.* **2024**, *23*, 100800. [CrossRef] [PubMed]
39. Lemke, S.; Vilcinskas, A. European Medicinal Leeches—New Roles in Modern Medicine. *Biomedicines* **2020**, *8*, 99. [CrossRef] [PubMed]
40. Montinari, M.R.; Minelli, S. From ancient leech to direct thrombin inhibitors and beyond: New from old. *Biomed. Pharmacother.* **2022**, *149*, 112878. [CrossRef] [PubMed]
41. Whitaker, I.S.; Oboumarzouk, O.; Rozen, W.M.; Naderi, N.; Balasubramanian, S.; Azzopardi, E.A.; Kon, M. The efficacy of medicinal leeches in plastic and reconstructive surgery: A systematic review of 277 reported clinical cases. *Microsurgery* **2012**, *32*, 240–250. [CrossRef] [PubMed]
42. Müller, C.; Mescke, K.; Liebig, S.; Mahfoud, H.; Lemke, S.; Hildebrandt, J.-P. More than just one: Multiplicity of Hirudins and Hirudin-like Factors in the Medicinal Leech, Hirudo medicinalis. *Mol. Genet. Genom.* **2016**, *291*, 227–240. [CrossRef] [PubMed]
43. Harvey, R.P.; Degryse, E.; Stefani, L.; Schamber, F.; Cazenave, J.P.; Courtney, M.; Tolstoshev, P.; Lecocq, J.P. Cloning and expression of a cDNA coding for the anticoagulant hirudin from the bloodsucking leech, Hirudo medicinalis. *Proc. Natl. Acad. Sci. USA* **1986**, *83*, 1084–1088. [CrossRef] [PubMed]
44. Rosa-Fernandes, L.; Rocha, V.B.; Carregari, V.C.; Urbani, A.; Palmisano, G. A Perspective on Extracellular Vesicles Proteomics. *Front. Chem.* **2017**, *5*, 102. [CrossRef] [PubMed]
45. Vagner, T.; Chin, A.; Mariscal, J.; Bannykh, S.; Engman, D.M.; Di Vizio, D. Protein Composition Reflects Extracellular Vesicle Heterogeneity. *Proteomics* **2019**, *19*, e1800167. [CrossRef] [PubMed]
46. Chitti, S.V.; Gummadi, S.; Kang, T.; Shahi, S.; Marzan, A.L.; Nedeva, C.; Sanwlani, R.; Bramich, K.; Stewart, S.; Petrovska, M.; et al. Vesiclepedia 2024: An extracellular vesicles and extracellular particles repository. *Nucleic Acids Res.* **2023**, *52*, D1694–D1698. [CrossRef] [PubMed]
47. Bandu, R.; Oh, J.W.; Kim, K.P. Mass spectrometry-based proteome profiling of extracellular vesicles and their roles in cancer biology. *Exp. Mol. Med.* **2019**, *51*, 1–10. [CrossRef] [PubMed]
48. Barnes, C.S.; Krafft, B.; Frech, M.; Hofmann, U.R.; Papendieck, A.; Dahlems, U.; Gellissen, G.; Hoylaerts, M.F. Production and Characterization of Saratin, an Inhibitor of von Willebrand Factor-Dependent Platelet Adhesion to Collagen. *Semin. Thromb. Hemost.* **2001**, *27*, 337–348. [CrossRef] [PubMed]
49. White, T.C.; Bernyl, M.A.; Robinson, D.K.; Yin, H.; DeGrado, W.F.; Hanson, S.R.; McCarthy, O.J.T. The leech product saratin is a potent inhibitor of platelet integrin α2β1 and von Willebrand factor binding to collagen. *FEBS J.* **2007**, *274*, 1481–1491. [CrossRef] [PubMed]
50. Tasiemski, A.; Vandenbulcke, F.; Mitta, G.; Lemoine, J.; Lefebvre, C.; Sautière, P.-E.; Salzet, M. Molecular Characterization of Two Novel Antibacterial Peptides Inducible upon Bacterial Challenge in an Annelid, the Leech Theromyzon tessulatum. *J. Biol. Chem.* **2004**, *279*, 30973–30982. [CrossRef] [PubMed]
51. Yuki, H.; Fishman, W.H. Purification and Characterization of Leech Hyaluronic Acid-endo-β-glucuronidase. *J. Biol. Chem.* **1963**, *238*, 1877–1879. [CrossRef]
52. Sun, R.; Fu, X.; Ai, R.; Huang, Z.; Li, H.; Tang, L.; Chen, H.; Zhang, X.; Zhao, F.; Lin, G. Feeding Strategy Shapes the Evolution of the Hyaluronidase Gene Family in Medicinal Leeches. *Ecol. Evol.* **2026**, *16*, e74049. [CrossRef] [PubMed]
53. Markwardt, F. Hirudin As Alternative Anticoagulant- A Historical Review. *Semin. Thromb. Hemost.* **2002**, *28*, 405–414. [CrossRef] [PubMed]
54. Warkentin, T.E.; Greinacher, A. The direct thrombin inhibitor hirudin. *Thromb. Haemost.* **2008**, *99*, 819–829. [CrossRef] [PubMed]
55. Cheng, B.; Liu, F.; Guo, Q.; Lu, Y.; Shi, H.; Ding, A.; Xu, C. Identification and characterization of hirudin-HN, a new thrombin inhibitor, from the salivary glands of *Hirudo nipponia*. *PeerJ* **2019**, *7*, e7716. [CrossRef] [PubMed]
56. Shi, P.; Wei, J.; You, H.; Chen, S.; Tan, F.; Lu, Z. Cloning, characterization, and heterologous expression of a candidate Hirudin gene from the salivary gland transcriptome of Hirudo nipponia. *Sci. Rep.* **2023**, *13*, 4943. [CrossRef] [PubMed]
57. Baskova, I.P.; I Nikonov, G. Destabilase: An enzyme of medicinal leech salivary gland secretion hydrolyzes the isopeptide bonds in stabilized fibrin. *Biokhimiia* **1985**, *50*, 424–431. [PubMed]
58. Zavalova, L.L.; Lazarev, V.N.; Levitsky, S.A.; Yudina, T.G.; Baskova, I.P. Destabilase-lysozyme of medicinal leech. Multifunctionality of recombinant protein. *Biochemistry* **2010**, *75*, 1173–1181. [CrossRef] [PubMed]
59. Marin, E.; Kornilov, D.A.; Bukhdruker, S.S.; Aleksenko, V.A.; Manuvera, V.A.; Zinovev, E.V.; Kovalev, K.V.; Shevtsov, M.B.; Talyzina, A.A.; Bobrovsky, P.A.; et al. Structural insights into thrombolytic activity of destabilase from medicinal leech. *Sci. Rep.* **2023**, *13*, 6641. [CrossRef] [PubMed]

60. Seemüller, U.; Meier, M.; Ohlsson, K.; Müller, H.-P.; Fritz, H. Isolation and Characterisation of a Low Molecular Weight Inhibitor (of Chymotrypsin and Human Granulocytic Elastase and Cathepsin G) from Leeches. *Hoppe-Seyler's Z. Für Physiol. Chem.* **1977**, *358*, 1105–1118. [CrossRef] [PubMed]
61. Renesto, P.; Ferrerlopez, P.; Chignard, M. Interference of Recombinant Eglin-C, A Proteinase-Inhibitor Extracted from Leeches, with Neutrophil-Mediated Platelet Activation. *Lab. Investig.* **1990**, *62*, 409–416. [PubMed]
62. Jo, S.-H.; Kim, S.-H.; Heo, S.C.; Cho, H.; Esfahani, I.J.; Park, S.-H. Exploring the Therapeutic Potential of Extracellular Vesicles Anchored to the Sea Cucumber Extracellular Matrix for Treating Atopic Dermatitis. *Biomater. Res.* **2025**, *29*, 0154. [CrossRef] [PubMed]
63. Susa, F.; Limongi, T.; Borgione, F.; Peiretti, S.; Vallino, M.; Cauda, V.; Pisano, R. Comparative Studies of Different Preservation Methods and Relative Freeze-Drying Formulations for Extracellular Vesicle Pharmaceutical Applications. *ACS Biomater. Sci. Eng.* **2023**, *9*, 5871–5885. [CrossRef] [PubMed] [PubMed Central]
64. Kim, J.H.; Lee, C.J.; Yu, Y.S.; Aryal, Y.P.; Kim, S.; Suh, J.Y.; Kim, J.Y.; Min, S.H.; Cha, I.T.; Lee, H.Y.; et al. Transcriptomic profiling and the first spatial expression analysis of candidate genes in the salivary gland of the East Asian medicinal leech, Hirudo nipponia. *Dev. Comp. Immunol.* **2024**, *154*, 105125. [CrossRef] [PubMed]

Disclaimer/Publisher's Note: The statements, opinions and data contained in all publications are solely those of the individual author(s) and contributor(s) and not of MDPI and/or the editor(s). MDPI and/or the editor(s) disclaim responsibility for any injury to people or property resulting from any ideas, methods, instructions or products referred to in the content.